

Analysis of As₂S₃-Ti: LiNbO₃ Taper Couplers Using Supermode Theory

Xin Xia, Yifeng Zhou, Christi K. Madsen

Department of Electrical and Computer Engineering, Texas A&M University, College Station, USA
Email: cmadsen@tamu.edu

Received October 16, 2012; revised November 14, 2012; accepted November 24, 2012

ABSTRACT

In this work, we develop a simulation method based on supermode theory and transfer matrix formalism, and then apply it to the analysis and design of taper couplers for vertically integrated As₂S₃ and Ti: LiNbO₃ hybrid waveguides. Test structures based on taper couplers are fabricated and characterized. The experimental results confirm the validity of the modeling method, which in turn, is used to analyze the fabricated couplers.

Keywords: Optical Waveguides; Couplers; Coupled Mode Analysis

1. Introduction

As study on integrated Optics proceeds, several schemes with regard to materials and structures were developed, such as silicon-on-insulator, chalcogenide glass waveguides, III-V semiconductor waveguides and titanium diffused waveguides. While different schemes have their own merits and shortcomings, reciprocal benefits can be obtained from integration of them, namely, the hybrid waveguides. For example, preliminary result was reported on As₂S₃-on-Ti: LiNbO₃ hybrid waveguide devices [1,2], which benefit from the high index contrast of As₂S₃ and easy connection with commercial single mode fibers. For integration of different waveguides, light coupling is the key. A directional coupler is the simplest functional device to couple light by transferring energy between two waveguides. However, in practice its coupling efficiency can be fairly low due to the phase mismatch and small tolerance to fabrication errors. Alternatively grating and taper couplers are used, and taper couplers are generally preferred owing to its simplicity in design and fabrication. Despite diverse forms, the general taper coupler is composed of two parallel waveguides placed in close proximity: one is uniform whereas at one end of the other one, the width is gradually varied. Two ends of the taper match the wave guiding properties of two waveguides, so the mode is transformed gradually from one into another during propagation in the taper. Although the principle is intuitively quite simple, the design in most cases is conservative because of the lack of precise modeling guidelines and accurate modeling tools [3]. A lot of theoretical study was carried out to investigate them, and different approaches were devel-

oped. Lee *et al.* proposed an equivalent waveguide concept employing a conformal mapping method, which was combined with the Beam Propagation Method (BPM) to conduct analysis [4]. In [3], tapered waveguides were analyzed by considering the whole taper as a succession of short linear taper fragments and modeling each of them using a two-dimensional BPM that solves directly the Helmholtz equation.

However, most of the early work focused on correcting simulation methods to improve the accuracy, and the underlying physical mechanism governing the power transfer was not described [5]. Therefore, few guidelines can be found for designers. Thus more and more researchers began to look into taper couplers from the angle of supermodes, *i.e.* local modes. In [5], Xia *et al.* defined and distinguished between the resonant coupling and adiabatic coupling from the view of supermodes [5]. Resonant couplers are compact and simple but highly sensitive to unavoidable variations during fabrication [5]. Adiabatic couplers, on the contrary, don't require exact control of taper length and gap, but need longer lengths [6]. Sun *et al.* conducted a series of studies on the behavior of supermodes in adiabatic couplers [6,7] and derived a mathematical expression of the shortest adiabatic tapers [6]. As such theoretical work contributed a lot to our understanding of taper couplers, the study on issues of practical application and modeling is still lacking. In practice, we often need to balance the taper length and the coupling efficiency, since we may not have sufficient space to fulfill the adiabatic condition, and we may want certain coupling efficiency that is not necessarily 100%. Mach-Zehnder interference filters, for example, typically use 3 dB couplers. Moreover, the mate-

rials and structures used may limit the coupling. Thus, there are a lot of efficient but non-adiabatic taper couplers desired in practice.

In published papers most simulations were conducted based on beam propagation method (BPM) [8]. BPM calculates the electromagnetic fields during light propagation process and gives distributions of electric and magnetic fields. It is highly accurate as long as certain assumptions are met. However, limited knowledge of underlying mechanism can be obtained from the simulation process, so it is widely used to as a means of examining the designed taper coupler instead of guiding the design at the first place. Alternatively, the modeling of taper couplers can be based on the concept of modes using the coupled mode theory, which can provide insights to the mode evolution in the coupler and thus provide immediate guidelines for design.

2. Modeling Methods

A taper coupler, which consists of two adjacent waveguides, can be regarded as a modified directional coupler. In each waveguide, only one mode is allowed to propagate. The coupled mode theory analyzes the coupled waveguides by taking one waveguide as the subject and studying the influence of the perturbation imposed by the presence of the other one. The supermode theory, however, views the coupled waveguides as a whole system, *i.e.* a composite two-waveguide structure, and studies the normalized local modes of the system, which are called supermodes. Nevertheless, both theories describe mode coupling for scenarios that coupled waveguides are invariable along the propagation direction. But the taper coupler is a varying structure where the width of one of the waveguides is constantly changing along the propagation direction. However, the coupler can be divided into a succession of infinitely short sections. The length of each section is so small that the width can be regarded as invariant. So the simulation of a taper coupler can be divided into two steps: modeling of individual divisions and a cascade of individual models. For each division, as the width is deemed constant, it is actually a simple directional coupler, in which there are fundamental supermode and first order supermode, named as even mode (E_e) and odd mode (E_o) respectively according to the symmetry of their field distributions. The total field is a linear combination of the even and odd mode.

If the propagation constants of modes in individual waveguides are the same, namely, they are phase matched, two lobes of even and odd mode have the same size. If two propagation constants are different, that is, the phases are mismatched, the symmetry of lobes of E_e and E_o is broken, and their shapes are different. When phase mismatch is large, two waveguides are effectively

decoupled: a wave propagating in either one is virtually unaffected by the existence of the other, and the supermodes of the composite structure just become those of the individual waveguides [9]. δ is defined as the difference of the propagation constants of two individual modes while β_c is for two supermodes in a similar way in (1):

$$\delta = \frac{\beta_2 - \beta_1}{2} \quad \text{and} \quad \beta_c = \frac{\beta_e - \beta_o}{2} \quad (1)$$

As shown in **Figure 1**, if δ is much smaller than 0, most energy of the even mode is located in waveguide 1 while if it is much larger than 0, most energy is located in waveguide 2. The opposite is true for the odd mode. So, the essence of taper coupling is to spatially transfer the energy of a supermode (even mode) from one waveguide to the other by designing the tapered waveguide so that δ sweeps from a negative value to a positive value while suppressing the coupling to the other supermode (odd mode) [6]. The larger scope δ covers, the more thorough the energy transfer is. Ideally, δ changes from negative infinity to positive infinity, whereas in practice, the scope is determined by the materials and structures.

Solving the coupled mode equations by substituting the general supermode solutions into them, we can obtain the expressions of supermodes and the relationship between the phase mismatch of supermodes (β_c) and that of individual modes (δ) [7]

$$\beta_c^2 = \delta^2 + \kappa^2 \quad (2)$$

As δ and β_c are known, the coupling strength κ [9] can be calculated. Then we have a complete mathematical description of the model with parameter δ , κ and β_c . Following the same method, models of all the divisions in the taper coupler can be built.

Subsequently, transfer matrix formalism is derived to cascade all the models based on coupled mode equations. In the matrix form, the solution to coupled mode equations is (3).

$$\begin{aligned} \begin{bmatrix} E_1(z) \\ E_2(z) \end{bmatrix} &= \begin{bmatrix} \cos(\beta_c z) + \frac{j\delta}{\beta_c} \sin(\beta_c z) \\ -\frac{j\kappa}{\beta_c} \sin(\beta_c z) e^{-i\delta z} - \frac{j\kappa}{\beta_c} \sin(\beta_c z) e^{i\delta z} \end{bmatrix} e^{-i\delta z} \\ &\cdot \begin{bmatrix} \cos(\beta_c z) - \frac{j\delta}{\beta_c} \sin(\beta_c z) \\ \end{bmatrix} e^{i\delta z} \begin{bmatrix} E_1(0) \\ E_2(0) \end{bmatrix} \end{aligned} \quad (3)$$

where $E_1(0)$ and $E_2(0)$ are the input electric fields in waveguide 1 and 2 respectively. Let $z = z_0$ and re-form the equation to obtain the expression of vector, let $z = z_0 + \Delta z$ to re-write (3), substitute the vector expression into it, and we arrive at the transfer matrix formalism relating the model at $z_0 + \Delta z$ to the model at

z_0 in (4).

$$\begin{aligned}
 & \begin{bmatrix} E_1(z_0 + \Delta z) \\ E_2(z_0 + \Delta z) \end{bmatrix} \\
 &= M(z_0 + \Delta z; z_0) \begin{bmatrix} E_1(z_0) \\ E_2(z_0) \end{bmatrix} M(z_0 + \Delta z; z_0) \\
 &= \left[\begin{bmatrix} \cos(\beta_c \Delta z) + \frac{j\delta}{\beta_c} \sin(\beta_c \Delta z) \\ -\frac{j\kappa}{\beta_c} \sin(\beta_c \Delta z) \end{bmatrix} e^{-i(\delta \Delta z)} \right. \\
 & \quad \left. -\frac{j\kappa}{\beta_c} \sin(\beta_c \Delta z) e^{-i[\delta(z_0 + \Delta z) + \delta z_0]} \right. \\
 & \quad \left. -\frac{j\kappa}{\beta_c} \sin(\beta_c \Delta z) e^{i[\delta(z_0 + \Delta z) + \delta z_0]} \right. \\
 & \quad \left. \cdot \begin{bmatrix} \cos(\beta_c \Delta z) - \frac{j\delta}{\beta_c} \sin(\beta_c \Delta z) \\ \frac{j\kappa}{\beta_c} \sin(\beta_c \Delta z) \end{bmatrix} e^{i(\delta \Delta z)} \right]
 \end{aligned} \tag{4}$$

Then by multiplying the matrices in order, the models are cascaded. As a result, the electric field at certain point z can be obtained from the known input $E_1(0)$ and $E_2(0)$. The algorithm is summarized in **Table 1**.

In step 2, due to the complexity of the waveguide structure, computer software FIMMWAVE (Photon Design Ltd.) is used to model each section, *i.e.*, to compute mode parameters. The film mode matching method is applied as the mode solver. It is good for structures consisting of large uniform areas, such as As_2S_3 rectangular waveguides. The resolution and the size of simulation window are tested to prevent artificial errors. Simulation

starts with uncoupled waveguides, and their eigen-modes are computed individually without the presence of the other one. The propagation constants of the Ti waveguide mode and the As_2S_3 waveguide mode are found to be β_1 and β_2 respectively. Then the model for the coupled system is built, and the even mode (β_e) and odd mode (β_o) are found, as **Figure 2** shows.

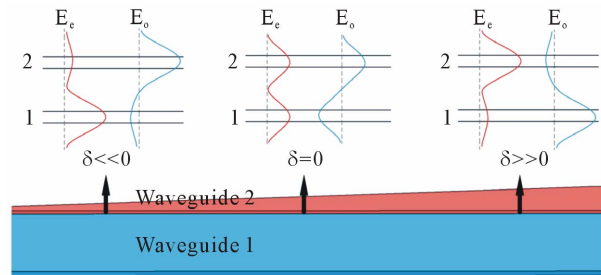


Figure 1. The supermodes of a taper coupler.

Table 1. Algorithm of modeling the taper coupler.

1	Discretize the taper coupler into a sequence of sufficiently small divisions;
2	Regard each section as a directional coupler and model it to obtain mode propagation constants $\beta_1, \beta_2, \beta_e$ and β_o , and compute δ, β_c and κ ;
3	Calculate individual transfer matrix of each division based on parameter δ, β_c and κ ;
4	Cascade all the divisions together by multiplying matrices in order;
5	Calculate the coupling efficiency.

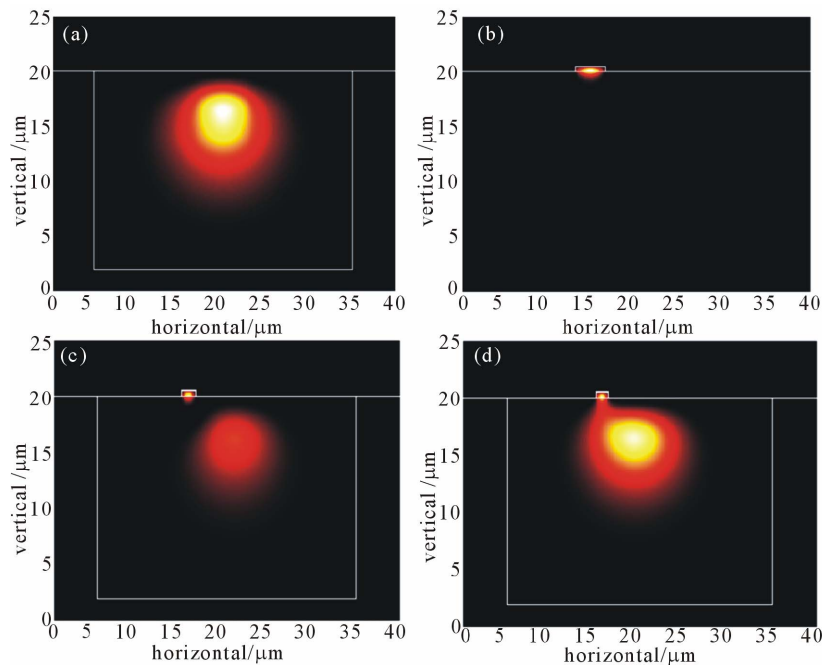


Figure 2. The fundamental mode of the Ti waveguide (a) and the As_2S_3 waveguide (b) and the odd (c) and even mode (d) of coupled waveguides.

The approximation of a width-varying waveguide with a sequence of width-constant waveguides is mathematically equivalent to the approximation of a continuous integral with a discrete summation, which induces error inevitably. As the matrices cascade, the previous error passes on, and combines with the error of the present one. Consequently, such accumulation of the errors will manifest at the end of the taper, even if very small error exists in intermediate models. Simulation experiments show that discretization spacing (Δz) is critical to the numerical error: the larger an error exists, the smaller the spacing needs to be, and the heavier the computation load is required. In order to reduce the error at the first place, the trapezoidal approximation algorithm

$\frac{X(i)+X(i+1)}{2} \cdot \Delta z$ is adopted to substitute left Riemann sum $X(i) \cdot \Delta z$ in (4) ($X = \beta_c, \delta$ and κ).

3. Simulation Results

The structure of an As_2S_3 -Ti: LiNbO_3 coupler is illustrated in **Figure 3**. A titanium diffused waveguide is formed in lithium niobate substrate (Ti: LiNbO_3). On substrate surface is a piece of tapered As_2S_3 rectangular waveguide, which is separated from the titanium diffused waveguide by a few microns. Both waveguides work in single mode condition. In Ti: LiNbO_3 fabrication process, the LiNbO_3 material under Ti pattern rises up from the substrate surface during titanium diffusion, resulting in a $0.1 \mu\text{m}$ high bump. In order to avoid the scattering loss caused by the rough surface of the bump, As_2S_3 waveguide is placed to the side of the bump (side coupling) instead of on the top. For simplicity, air cladding is used. The height of As_2S_3 waveguide is 470 nm . The final width of As_2S_3 waveguide is determined to be $3.5 \mu\text{m}$, in order to have a good mode confinement in the As_2S_3 waveguide.

As the width of As_2S_3 taper varies, the mode propaga-

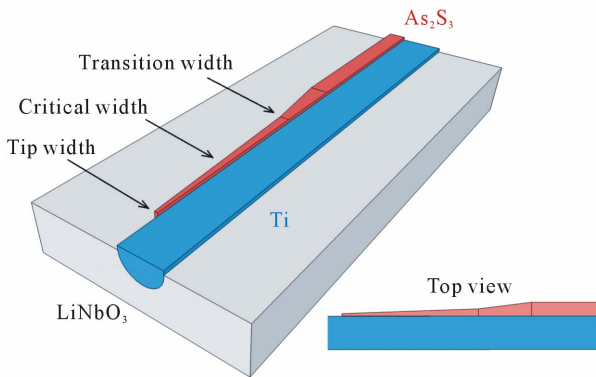


Figure 3. Configuration of an As_2S_3 -Ti: LiNbO_3 taper coupler (two-stage taper design). The inset picture shows a top view.

tion constants in each section are plotted against the average width of that section in **Figure 4**.

We see that the propagation constant of As_2S_3 mode increases gradually as its width becomes larger whereas the Ti mode remains constant due to the invariable Ti waveguide width. The propagation constant of the even mode coincides with that of the Ti mode first and then gradually follows the trend of the As_2S_3 mode. On the contrary, for odd mode, the propagation constant goes from the As_2S_3 mode to the Ti mode. During this process, there is a point that the propagation constants of the As_2S_3 mode and the Ti mode are equal, corresponding to the point that the phase mismatch δ equals to 0. From the graph, it is the point where the β - As_2S_3 and β -Ti curves cross, corresponding to the width of $1.47 \mu\text{m}$, called as critical width. It is the critical point where two waveguides are phase matched, and the energy is equally distributed in two waveguides for both even and odd mode. In other words, it can be regarded as the mid-point of mode coupling process from Ti waveguide to As_2S_3 waveguide.

As the width of the As_2S_3 waveguide increases, the increasing rate of propagation constant β_2 gets smaller. That means the phase mismatch δ , the difference between the propagation constants of two waveguides, will eventually cease to grow. The normalized phase mismatch γ [6] is introduced to characterize such variation [6], as shown in (5) and plotted in **Figure 5**.

$$\gamma = \frac{\delta}{\kappa} \tag{5}$$

Among various types of taper geometries, the linear taper is most straightforward and provides insights into

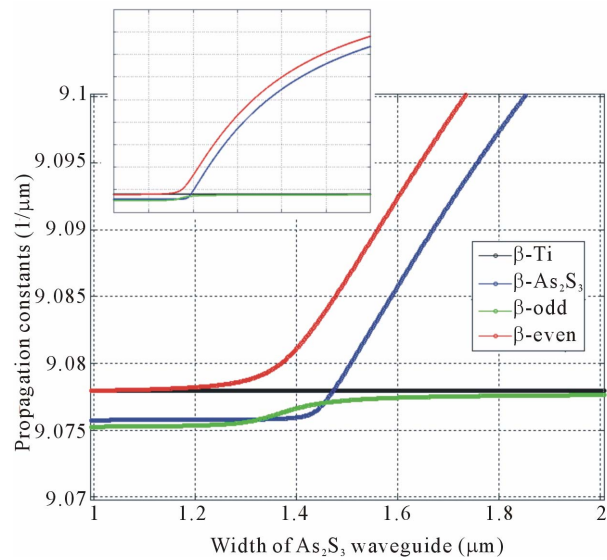


Figure 4. The propagation constants of four modes. The inset picture shows them in a larger scale (from $0.6 \mu\text{m}$ to $4 \mu\text{m}$).

the general taper design. **Figure 6** shows the coupling efficiency of linear tapers of different lengths, with width varying from 1.0 μm to 3.5 μm .

The squares stand for the coupling efficiency and the bars represent the magnitude of oscillation. There is an optimum point that the maximum coupling efficiency reaches 96% when the length is 5 mm. The inset curve shows the percentage of energy coupled as light propagates through a 5 mm long linear taper. We can see that it consists of a monotonically ascending part and a subsequent oscillation part. The coupling is mostly contributed by the former part while the latter is due to resonance effects.

For the even mode, the larger γ is, the more energy is located in As_2S_3 waveguide and the less in Ti waveguide, while it is vice versa for the odd mode. Since the even mode is the mode to couple, the energy remaining in Ti

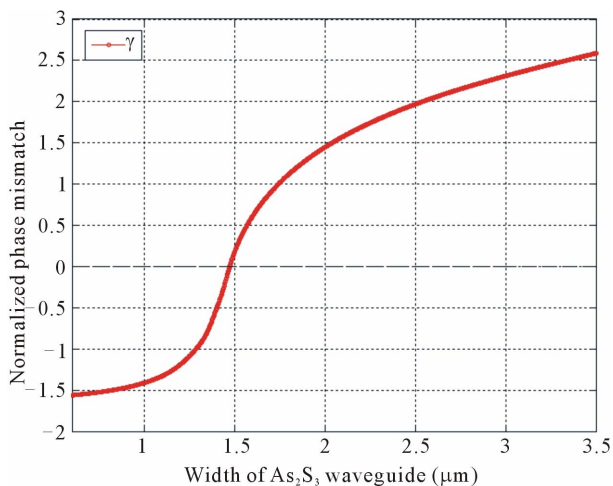


Figure 5. γ of the As_2S_3 -Ti: LiNbO₃ coupler.

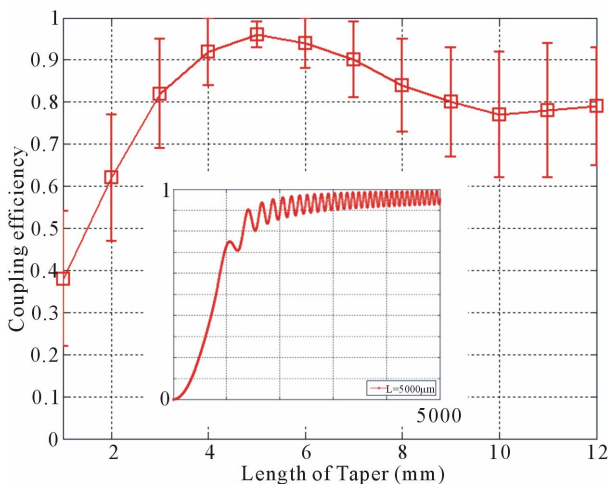


Figure 6. Coupling efficiency for tapers of different length, with the inset figure showing the coupling process of a 5 mm long taper, *i.e.*, the coupling efficiency versus the location along the taper.

waveguide imposes an ultimate limit to the coupling efficiency. From the curve of γ in **Figure 5**, we learn that at the end of the taper, γ is 2.59. Because γ is not large enough, there is still a coupling between two waveguides. Such coupling deteriorates the coupling efficiency and causes it to oscillate. The behavior of the coupler in this region is similar to that of a resonant coupler. As a result, a certain amount of energy flows back and forth between the two waveguide modes. From the view of supermode theory, the oscillation is a result of beating between the even and odd modes. Although the even mode is desired, the coupling of the odd mode is not completely suppressed, for example, if the length of the taper is not long sufficiently according to the adiabatic criterion in [6]. When the odd mode propagates in the taper, there is coupling between the even and odd modes and a small amount of energy flows back and forth constantly. Since at the end of taper, the majority of the energy of the even mode is in As_2S_3 waveguide and that of the odd mode is in Ti waveguide, there is a constant energy flow between two waveguides, and consequently the coupling efficiency oscillates.

In the presence of mode beating, it is not necessarily the longer taper, the better coupling. There exists an optimum length for a taper with fixed width variation: if it is shorter than that, the mode is under-coupled since it is far away from the adiabatic criterion for 100% coupling; if considerably longer than that, the coupling efficiency is degraded by the resonant effect, as **Figure 6** shows. In order to reduce the problem of mode beating, we must enlarge γ , either by increasing the phase mismatch δ or by decreasing the coupling strength κ . δ is limited by the property of the materials whereas κ can be controlled by the structure. For example, κ can be reduced by introducing a gap between As_2S_3 waveguide and Ti waveguide.

Although the coupling efficiency can be as high as 96%, it takes quite a few millimeters to get a decent coupling efficiency for linear tapers, which is not acceptable for ultra-compact design. According to the above analysis, efficient coupling takes place in the first part of taper where As_2S_3 waveguide expands across the critical width and correspondingly the phase mismatch δ changes from a negative value to a positive one. That contributes to efficient coupling and we want it to be sufficiently long. Once most of energy has entered As_2S_3 waveguide, the rest of the taper can be shortened. As a consequence, we have arrived at a two-stage taper (**Figure 3**). Furthermore, since the end width of the first stage (transition width) can now be a much smaller value, the rate of width change is reduced largely. Simulation shows that for the first part of a two-stage taper, if the width varies from 1.0 μm to 1.6 μm (have some leeway for fabrication deviations) in the length of 2 mm, the width increasing rate is

3×10^{-4} , which is equivalent to an 8.3 mm long linear taper. Along with a 1 mm long second part, with width varying from 1.6 μm to 3.5 μm , the total length is 3 mm. The coupling efficiency can still reach above 90%, whereas the total length is reduced by 64%.

4. Experiments

To test As_2S_3 -Ti: LiNbO_3 taper coupler design, S-shaped structures are fabricated and tested on a near IR measurement setup. As shown in **Figure 7**, it is composed of two taper couplers and an S-shaped As_2S_3 waveguide to connect them. The taper couplers follow the two-stage taper coupler design.

The device is fabricated using photolithography and dry-etch technology. The substrate LiNbO_3 is a birefringence crystal with refractive index $n_o = 2.2119$ and $n_e = 2.1386$ ($\lambda = 1531$ nm), placed in x-cut, y-propagation manner. The titanium diffused waveguide is fabricated through sputtering of a 95 nm thick titanium layer, patterning into 7 μm wide strip with photolithography and reactive ion etching (RIE), diffusion for 9 hours at 1025°C and optical polishing on end-facets.

For As_2S_3 waveguide fabrication, a layer of 0.47 μm thick As_2S_3 film is deposited on the titanium waveguide sample using an RF sputtering system, along with a protective layer of SiO_2 and Ti, which protects the As_2S_3 from being dissolved by commercial alkaline-based developers. Then the projection photolithography is carried out, and the 1.0 μm wide taper tip can be produced, nevertheless the subsequent hardbake causes an expansion to certain degree. After that, the Ti- SiO_2 - As_2S_3 stack is etched through to the substrate by RIE. And Ti- SiO_2 is removed in diluted hydrofluoric solution at last.

The hardbake time is prolonged in order to obtain smoother sidewalls by the resist reflow process, which, however, causes an expansion of As_2S_3 waveguide to certain degree, up to 0.5 μm . The average tip width (*i.e.* the initial width) of tapered As_2S_3 waveguide after fabrication is 1.3 μm . Depending on the process conditions

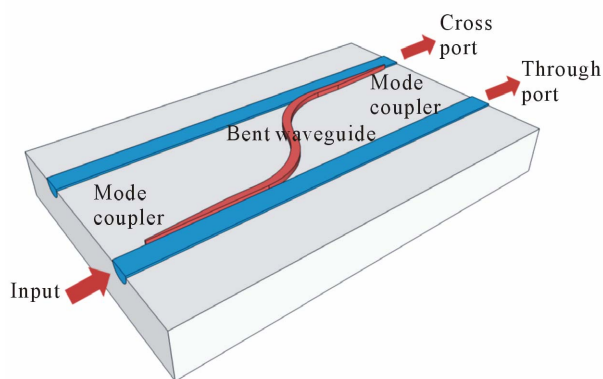


Figure 7. S bend structures for testing taper couplers.

such as exposure and development, it can be smaller or larger than that. Simulation study on the influence of the tip width variation for two-stage tapers is shown in **Figure 8**, along with the coupling curve of a two-stage taper coupler.

Measurement results confirm the function of the taper coupler following the design in section III (**Table 2**).

Generally, the cross port accounts for 50% to 90% of the total output power. Neglecting the excess loss caused by propagation in the low-loss As_2S_3 and Ti waveguides, the average coupling efficiency is 73.2%. However, prior to extracting the precise coupling efficiency, the propagation loss and bending loss in As_2S_3 waveguide have to be calibrated first. Many experiments need to be done for that, and the work is still ongoing.

Instead of working at a single wavelength, these practical taper couplers are designed to work for a wavelength range. Accordingly, their coupling behaviors in frequency domain are studied. The measured spectrum at the cross port is presumably to have the same trends of the coupling spectrum, with an offset from the exact values. That offers the information of taper couplers in the frequency domain and can be used as another means to test our simulation method. The typical measured spectrum, along with simulation results is shown in **Figure 9**. In simulation the wavelength is scanned correspondingly from 1520 nm to 1600 nm, at the interval of 2 nm. The results show that, though the taper coupler exhibits certain degree of wavelength dependency, it has high coupling efficiency over a broad bandwidth.

From the curve, we can see that the period of oscillation is less than 10 nm, and longer wavelengths have a

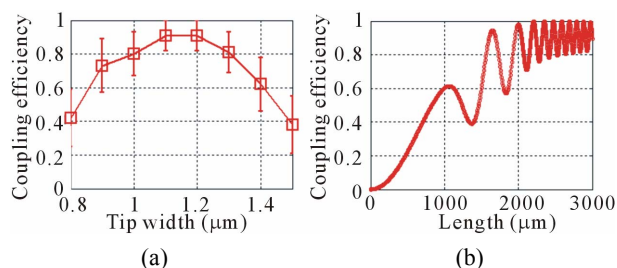


Figure 8. Influence of tip width variation (a) and the coupling process of a two-stage taper (b).

Table 2. Measurement results.

Sample	Cross (dB)	Through (dB)	Cross in Total (%)
1	-12.5	-31	98.6
2	-13	-26	95.2
3	-8.8	-7.8	44.3
4	-12.3	-16.4	72
5	-15.9	-16.9	55.7

larger oscillation period than shorter wavelengths: both are captured by the simulation. The oscillation of the coupling curve is a strong indication of mode beating while the phenomenon that longer wavelengths have a slightly larger oscillation period possibly comes from waveguide dispersion: the wavelength-dependent propagation constant. Simulation shows that when the wavelength varies from 1530 nm to 1540 nm, the confinement of the mode in As₂S₃ waveguide changes from 0.4536 to 0.4459 and the effective index changes from 2.2345 to 2.2331. Consequently, the propagation constant changes from 9.1763 to 9.1110, decreasing by 0.7%. From the plot of γ in **Figure 10**, we can learn that different wavelengths have different critical widths, which shifts to a larger value as the wavelength increases. Such change

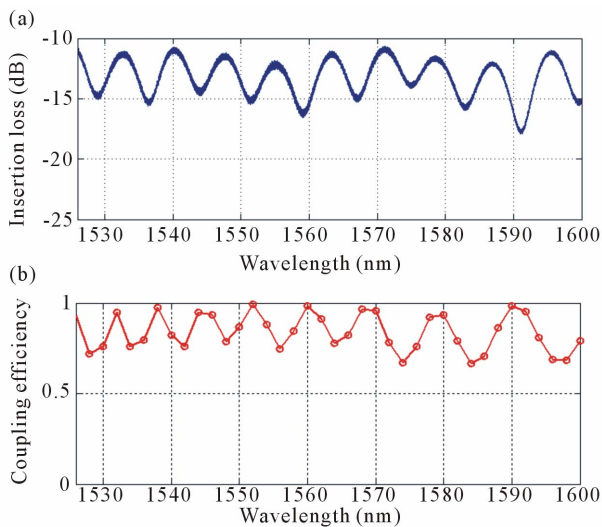


Figure 9. Measured (a) and simulated (b) coupling spectra of taper coupler with tip width = 1.3 μm .

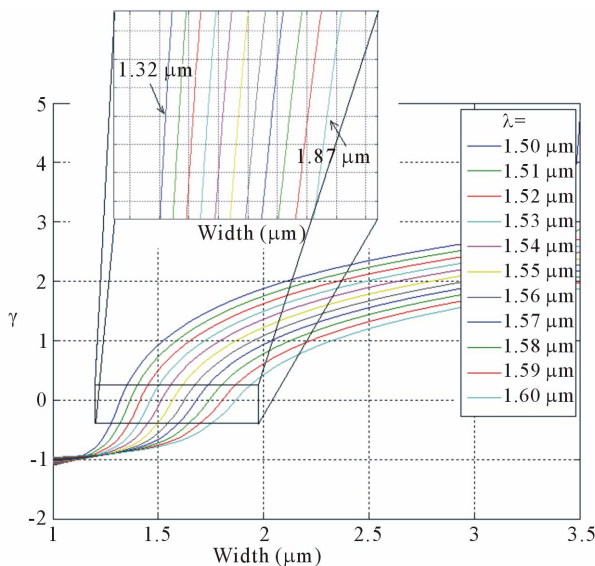


Figure 10. γ of the taper couplers at different wavelengths.

makes the mode at different wavelengths see the taper coupler slightly different, and the energy transfer does not take place at the same location: the mode of shorter wavelength couples before that of a longer wavelength does. From the inset plot of γ in **Figure 10**, we also see that as wavelength increases, the rate of shift increases, confirming the presence of dispersion.

Because of a 0.3 μm expansion during fabrication, the average tip width of tapered As₂S₃ waveguide is 1.3 μm , and accordingly the transition width is 1.9 μm . Whether it is smaller or larger than that is dependent on the process conditions, which is hard to control and manifested in the measured coupling spectra, as shown in **Figures 11(a)** and **12(a)**. Models are built to analyze them, in **Figures 11(b)** and **12(b)**. In **Figure 11**, there is a drop in coupling efficiency in long wavelength region, while the model shows if the tip width is reduced to 1.2 μm , correspondingly the end width of the first stage is 1.8 μm , such a coupling spectrum will be resulted. The phenomenon can be understood from the plot of γ in **Figure 10**: at the wavelength of 1600 nm, the critical width is read to be 1.87 μm , which is larger than the actual transition width (1.8 μm). Hence the transfer of the energy has not completed yet at the end of the first stage, and resumes at the second stage where the width varies very fast, and considerable energy is coupled to odd mode. Consequently, the coupling efficiency drops.

Similarly, the model explains the drop of coupling efficiency in the short wavelength region for **Figure 12**. Provided that the tip width is larger, e.g. 1.4 μm , for short wavelengths such as 1525 nm, the critical width is 1.32 μm , which is smaller than the initial tip width. As a result, the odd mode is excited at the input of the taper coupler, and the coupling efficiency in this wavelength region is degraded, as shown in the curve.

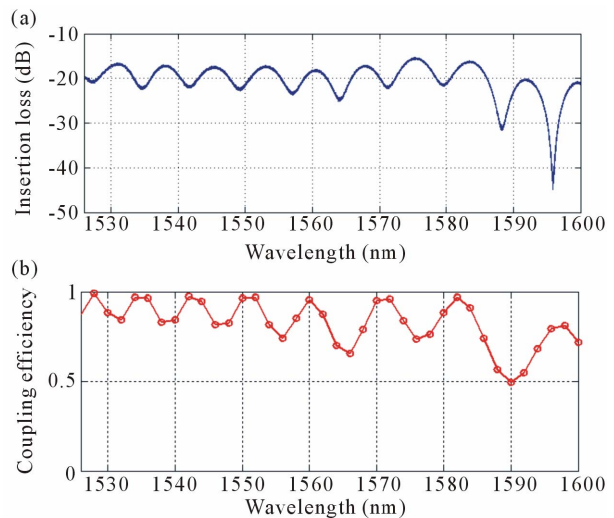


Figure 11. Measured (a) and simulated (b) coupling spectra of taper coupler with tip width = 1.2 μm .

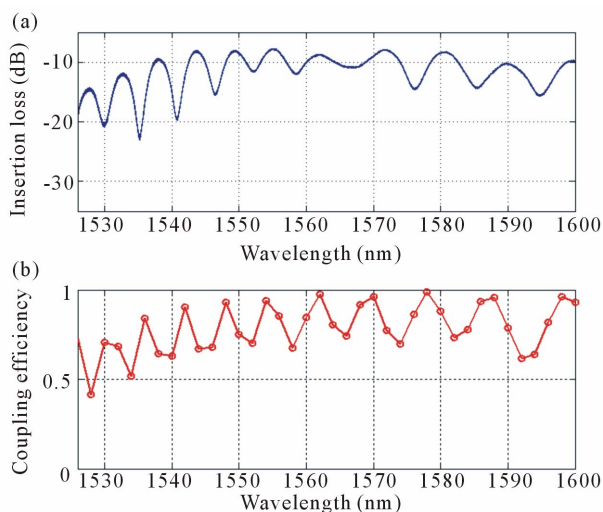


Figure 12. Measured (a) and simulated (b) coupling spectra of taper coupler with tip width = 1.4 μm .

From the above analysis, we see a tradeoff between the applicable wavelength range and the design parameters, which, on the other side, provides a way of controlling the frequency domain behavior of taper couplers: by adjusting the transition width between two stages we can cut off longer wavelengths and by changing the tip width we can suppress the coupling of shorter wavelengths.

5. Conclusion

A modeling method for taper couplers is developed and applied to the study of As_2S_3 -Ti: LiNbO_3 taper couplers, which are generally not adiabatic but highly efficient in terms of practical use. Simulations show that for those practical tapers, both adiabatic coupling and resonant coupling play an important role. There exists an optimum taper design with respect to the tip width, end width and length. A two-stage taper design can largely reduce the total length of the taper by 64% while keeping high coupling efficiency above 90%. Following the guidelines, test structures are fabricated. The measurement results agree with the simulation results well, suggesting a good coupling efficiency. Frequency domain analysis shows that the taper couplers work for a range of wavelengths, which can be controlled by adjusting the transition width and the tip width.

6. Acknowledgements

The authors would like to thank William Tim Snider and Travis E. James for the help in fabrication. This publication was supported by the Pennsylvania State University Materials Research Institute Nanofabrication Lab and National Science Foundation Cooperative Agreement No. 0335765, National Nanotechnology Infrastructure Network, with Cornell University.

REFERENCES

- [1] M. E. Solmaz, *et al.*, "Compact Bends for Achieving Higher Integration Densities for LiNbO_3 Waveguides," *IEEE Photonics Technology Letters*, Vol. 21, No. 9, 2009, pp. 557-559. [doi:10.1109/LPT.2009.2014569](https://doi.org/10.1109/LPT.2009.2014569)
- [2] M. E. Solmaz, *et al.*, "First Demonstration of an As_2S_3 -on- LiNbO_3 Ring Resonator," *Conference on Optical Fiber Communication—Includes Post Deadline Papers*, San Diego, 22-26 March 2009, pp. 1-3.
- [3] J. Haes, *et al.*, "Design of Adiabatic Tapers for High-Contrast Step Index Waveguides," *Linear and Nonlinear Integrated Optics*, Lindau, 11-13 April 1994, pp. 685-693.
- [4] C.-T. Lee, *et al.*, "Design and Analysis of Completely Adiabatic Tapered Waveguides by Conformal Mapping," *Journal of Lightwave Technology*, Vol. 15, No. 2, 1997, pp. 403-410.
- [5] F. Xia, *et al.*, "Photonic Integration Using Asymmetric Twin-Waveguide (ATG) Technology: Part I-Concepts and Theory," *IEEE Journal of Selected Topics in Quantum Electronics*, Vol. 11, No. 1, 2005, pp. 17-29. [doi:10.1109/JSTQE.2004.841466](https://doi.org/10.1109/JSTQE.2004.841466)
- [6] X. Sun, *et al.*, "Adiabaticity Criterion and the Shortest Adiabatic Mode Transformer in a Coupled-Waveguide System," *Optics Letters*, Vol. 34, No. 3, 2009, pp. 280-282. [doi:10.1364/OL.34.000280](https://doi.org/10.1364/OL.34.000280)
- [7] A. Yariv and X. Sun, "Supermode Si/III-V Hybrid Lasers, Optical Amplifiers and Modulators: A Proposal and Analysis," *Optics Express*, Vol. 15, No. 15, 2007, pp. 9147-9151. [doi:10.1364/OE.15.009147](https://doi.org/10.1364/OE.15.009147)
- [8] J. Haes, *et al.*, "A comparison between Different Propagative Schemes for the Simulation of Tapered Step Index Slab Waveguides," *Journal of Lightwave Technology*, Vol. 14, No. 6, 1996, pp. 1557-1569.
- [9] J.-M. Liu, "Coupling of Waves and Modes," In: J.-M. Liu, Ed., *Photonic Devices*, Cambridge University Press, Cambridge, 2005, p. 1052.